EVALUATION OF PRESSURE EFFECT ON HEAT TRANSFER COEFFICIENT AT THE METAL- MOLD INTERFACE FOR CASTING OF A356 ALALLOY

A. Fardi Ilkhchy, N. Varahraam,* and P. Davami

* n_varahraam@razi-center.net

Received: December 2011

Accepted: January 2012

¹ Department of Materials Scince and Engineering, Sharif University of Technology, Tehran, Iran.
 ² Razi Metallurgical Research Center, Tehran, Iran.

Abstract: During solidification and casting in metallic molds, the heat flow is controlled by the thermal resistance at the casting-mold interface. Thus heat transfer coefficient at the metal- mold interface has a predominant effect on the rate of heat transfer. In some processes such as low pressure and die-casting, the effect of pressure on molten metal will affect the rate of heat transfer at least at initial steps of solidification. In this study interfacial heat transfer coefficient at the interface between A356 alloy casting and metallic mold during the solidification of casting under pressure were obtained using the IHCP (Inverse Heat Conduction Problem) method. Temperature measurements are then conducted with the thermocouples aligned in the casting and the metallic mold. The temperature files were used in a finite-difference heat flow program to estimate the transient heat transfer coefficients. The peak values of heat transfer coefficient obtained for no pressure application of A356 alloy is 2923 ($\frac{w}{m^2k}$) and for pressure application is 3345 ($\frac{w}{m^2k}$). Empirical equation, relating the interfacial heat transfer coefficient transfer coefficient transfer dent of pressure application at transfer coefficient transfer coefficient transfer and for pressure application of A356 alloy is 2923 ($\frac{w}{m^2k}$).

Keywords: Air Gap, Metal/Mold Interfacial, Permanent Mold, Heat Transfer Coefficient, IHCP Method.

1. INTRODUCTION

It is well-known that solidification of a cast part, the condition of the contact interface between a mold and a casting, has great influence on cooling rate and freezing time. In the case of permanent mold casting, due to higher cooling rate as compared to sand casting, it need better control over the heat transfer and solidification phenomena to improve the mechanical properties and soundness of the casting[1].

The casting does not contact ideally with the mold and there is a considerable thermal resistance between them. It is necessary to know how the heat transfer coefficients varies with time after pouring. Several studies have attempted to quantify the transient interfacial metal-mold heat transfer coefficient, hi, emphasizing different factors which affect heat flow across such interfaces during solidification [2,5,6,7,8].

These factors include the thermo-physical properties of contacting materials, casting geometry, orientation of casting–Die mold interface with respect to gravity (contact

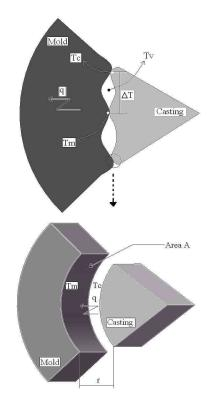


Fig.1. Representation of heat flow across permanent mold-casting interface.

pressure), mold temperature, pouring temperature, roughness of mold contacting surface, mold coatings, etc. [9,10,11].

When metal and mold surfaces are brought into contact an imperfect junction is formed. While uniform temperatures gradients can exist in both metal and mold, the junction between the two surfaces creates a temperature drop, this means that molten metal becomes very viscous, in the early stage of solidification, and later completely solidifies. During this process, a gap is formed between the casting metal and the mould. formation of This gap due to the following reasons. First, the thermal expansion coefficients of the molten metal and mould are different. Second, some of the air initially is trapped in the mould cavity and cannot escape through the mould. Third, the coatings on the inner surface of the mould may evaporate or burn due to high temperature, which contributes as an additional source of gases between the metal and mould. These factors affect the size of the gap formed [9,12]. Figure 1 shows a schematic representation of two contacting surfaces.

2. GOVERNING EQUATIONS

The heat flow across the metal-mold interface can be characterized by a macroscopic average metal/mold interfacial heat transfer coefficient (h_i) given by[3,4]:

$$h_i = \frac{q}{A(T_c - T_M)} \tag{1}$$

Where q is the average heat flux across the interface; T_C and T_M are casting and mold surface temperatures. Development of the used mathematical model is based on the general equation of heat conduction [13] expressed in cylindrical coordinate:

$$\rho C_P \frac{\partial T}{\partial t} = \frac{1}{r} \frac{\partial}{\partial r} \left(kr \frac{\partial T}{\partial r} \right) + \frac{1}{r^2} \frac{\partial}{\partial \varphi} \left(k \frac{\partial T}{\partial \varphi} \right) + \frac{\partial}{\partial z} \left(k \frac{\partial T}{\partial z} \right) + \dot{q}$$
(2)

Where ρ is density, C_P is heat capacity, k thermal conductivity of the cast metal, \dot{q} the heat

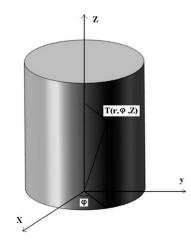


Fig. 2. Cylindrical coordinate system.

source and r, z and φ are the cylindrical coordinates represented in Figure 2.

Considering radial flow of heat as dominate heat transfer direction, equation (1) can be reduced to one-dimensional form. Thus, the direction z of heat extraction can be neglected, once it is not significant regarding the heat flow in the r and f directions. In the case of ingots with a symmetrical section, the heat flow in the φ direction can also be neglected, resulting in a simplified equation. Therefore, the one dimensional transient heat equation in cylindrical coordinates will be[3]:

$$\rho C_P \frac{\partial T}{\partial t} = \frac{k}{r} \frac{\partial}{\partial r} \left(r \frac{\partial T}{\partial r} \right) + \dot{q}$$
(3)

The term of the heat generation of energy (\dot{q}) in the unsteady state condition is[3]:

$$\dot{q} = \rho . \Delta H_m . \frac{\partial f_s}{\partial t} \tag{4}$$

 ΔH_m is the latent heat of fusion and ∂f_s is the fraction of solid formed during the phase transformation which[3]:

$$\frac{\partial f_s}{\partial t} = \frac{\partial f_s}{\partial T} \cdot \frac{\partial T}{\partial t}$$
(5)

For short or long freezing range alloys, the latent heat evolution was taken into account by using Scheil's equation until the remaining liquid reached the eutectic composition[3]:

$$f_s = 1 - \left(\frac{T_m - T}{T_m - T_L}\right)^{\left(1/(k_0 - 1)\right)}$$
(6)

Where k_0 is the distribution coefficient, T_m and T_L are melting point and liquidus temperature. By simplifying equations 3 to 6 we have:

$$\rho C_P \frac{\partial T}{\partial t} = \frac{1}{r} \frac{\partial}{\partial r} \left(k. r \frac{\partial T}{\partial r} \right) + \rho. \Delta H_m. \frac{\partial f_s}{\partial T}. \frac{\partial T}{\partial t}$$
(7)

Expanding the partial derivatives in relation to the radius and considering the material as isotropic, rearranging equation (7), it follows that[9,12]:

$$\rho \left(C_P - \Delta H_m \cdot \frac{\partial f_s}{\partial T} \right) \frac{\partial T}{\partial t} = k \cdot \left(\frac{\partial^2 T}{\partial r^2} + \frac{1}{r} \frac{\partial T}{\partial r} \right)$$
(8)

Where:

$$\acute{C} = \left(C_P - \Delta H_m \cdot \frac{\partial f_s}{\partial T}\right) \tag{9}$$

and the cylindrical coordinates equation is reduced to:

$$\frac{\partial T}{\partial t} = \frac{k}{\rho \acute{C}} \cdot \left(\frac{\partial^2 T}{\partial r^2} + \frac{1}{r} \frac{\partial T}{\partial r} \right)$$
(10)

Using the finite difference method (FDM) for the development of equation (8), we have:

$$T_{i}^{n+1} = \frac{k \cdot \Delta t}{\rho_{i} \hat{C}_{i}} \left[\frac{T_{i-1}^{n} - 2T_{i}^{n} + T_{i+1}^{n}}{\Delta r^{2}} + \frac{1}{r_{i}} \cdot \left(\frac{T_{i+1}^{n} - T_{i-1}^{n}}{2\Delta r} \right) \right] + T_{i}^{n}$$
(11)

For i≠ 0

$$T_{i}^{n+1} = \frac{\Delta t}{\rho_{i} \cdot \hat{C}_{i} \cdot r_{i} \cdot \Delta r^{2}} \left[k \cdot r_{i-\frac{1}{2}} \cdot (T_{i-1}^{n} - T_{i}^{n}) + k \cdot r_{i+1} \cdot \left(T_{i+\frac{1}{2}}^{n} - T_{i}^{n} \right) \right] + T_{i}^{n}$$
(12)

Where the subscript (*i*) represents the location of the element in the finite difference mesh and (n+1), the instant in that the nodal temperature is being calculated. Considering the metal/mold interface, the following thermal balance can be

applied:

$$T_{M/m}^{n+1} = \frac{\Delta t}{\rho_i \cdot \hat{C}_i \cdot r_m \cdot \Delta r} \left[h. r. (T_a^n - T_m^n) + k. r_{m-\frac{1}{2}} \cdot \left(\frac{T_{m-1}^n - T_m^n}{\Delta r} \right) \right] + T_{M/m}^n$$
(13)

where T_a , is ambient temperature r_m , it is external radius of the cylindrical ingot; $T_{M/m}$, is the metal/mold interface temperature and h, it is the overall heat transfer coefficient between the casting surface and air.

3. DETERMINATION OF INTERFACIAL HEAT TRANSFER COEFFICIENTS

The heat flow across the metal-mold interface can be characterized by Eq. (1) and h can be determined provided that all the other terms of the equation, namely q, T_C and T_M , are known [6]. difficult to measure these However, it is parameters because accurate locating of the thermocouples of finite mass at the interface is not an easy task, and they can distort the temperature gradient at the interface. To overcome this experimental impediment, the methods of calculation of h_i existing in the literature are based on knowledge of other conditions, such as temperature histories at interior points of the casting or mold, together with mathematical models of heat flow during solidification. Among these methods, those based on the solution of the inverse heat conduction problem have been widely used in the quantification of the transient interfacial heat transfer[14].Since solidification of a casting involves both a change of phase and temperature variable thermal properties, the inverse heat conduction becomes nonlinear. Most of the methods of calculation of time-dependent hi existing in literature are based on numerical techniques, generally known as methods of solving the inverse heat conduction problem [15, 16, 17, 18]. IHCP method is based on a complete mathematical description of physics of the process, supplemented with experimentally obtained temperature measurements in metal and/or mold. The inverse problem is solved by adjusting parameters in the mathematical

description to minimize the difference between the model computed values and the experimental measurements. Nonlinear estimation technique was used by Beck [13] for the numerical solution of this class of problem.

It has advantage over the other numerical in that Beck studied the problem from the standpoint, effective treatment of experimental data, taking into account inaccuracies concerning the locations of thermocouples places. statistical errors in temperature measurement and uncertainty in material properties. In the present work, a similar procedure used to determine the value of h_i which minimizes an objective function defined by equation14:

$$F(h) = \sum_{i=1}^{n} (T_{est} - T_{exp})^2$$
(14)

where T_{est} and T_{exp} are, respectively, the estimated and *n* experimentally measured temperatures at various thermocouples locations and times, and n is the iteration stage. A suitable initial value of h_i is assumed and with this value, the temperature of each reference location in casting and mold at the end of each time interval Δt is simulated by using an explicit finite difference technique. The correction in h_i at each iteration step is made by a Δh_i value, and new temperatures are estimated $[T_{est} (h_i + \Delta h_i)$ or $T_{exp} (h_i - \Delta h_i)]$. With these values sensitivity coefficients (() are calculated in each iteration is, given by:

$$\phi = \frac{T_{est}(h_i - \Delta h_i) - T_{est}(h_i)}{\Delta h_i}$$
(15)

The sequence of the equations involves the calculation of the sensitivity coefficients for measured temperatures. The assumed value of h is corrected using equation 16:

$$h_i(new) = h_i(old) \pm \Delta h_i \tag{16}$$

The above-indicated procedure is repeated for a new h, and is continued until

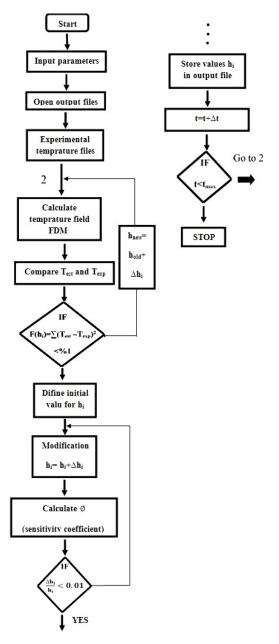


Fig. 3. Flow chart for the determination of metal–mold heat transfer coefficients.

$$\frac{\Delta h_i}{h_i} \tag{17}$$

Calculation of h as a function of time is continued until the end of the desired period. The flow chart, shown in Figure 3, gives an overview of the solution procedure.



Fig. 4. Parts of the mold.

4. EXPERIMENTAL DETAILS

The material used for the present study was commercial A356 Al alloy. The chemical composition of the used alloy in this study is listed in Table 1.

 Table 1. Chemical composition of the commercial A356 aluminium alloy.

Component	Si	Mg	Mn	Fe	Cu	Zn	Ti	Al
(wt%)	7.1	0.4	0.1	0.16	0.04	0.01	0.11	bal

 Table 2. Casting and mold properties used for simulating of heat transfer

of field transfer							
properties	Metal	Mold					
$k_{s} (Wm^{-1} K^{-1})$	185	46					
$k_1 (Wm^{-1} K^{-1})$	180	-					
$C_{s} (J. kg^{-1}.K^{-1})$	1084	527					
$C_1 (J. kg^{-1}.K^{-1})$	1130	-					
ρ_{z} (kg. m ⁻³)	2600	7860					
ρ_l (kg. m ⁻³)	2500	-					
$\Delta H_m(J. Kg^{-1})$	421	-					
K ₀	0.17	-					
$T_{s}(^{0}C)$	609	-					
$T_1 (^0C)$	559	-					
$T_o((^{0}C)$	750	300					

Mold was made of carbon steel. The selected casting and mold for experimentation, and the employed thermo-physical properties are summarized in Table 2.

Due to provide easier ejection of the casting from the mold after each test, The mold was built in three parts[19], Figure 4. The cavity of the mold was 50mm ×180mm.

In order to evaluate the temperature change during the solidification process, five sheath thermocouples (3.5mm⁻) were used, as shown in Figure 5. Two chromel-alumel thermocouples were inserted into two holes drilled to a depth of 10 and 15mm, shown as locations A and B and three holes were pierced in the bottom of the mold for inserting thermocouples at location C, D and E in the casting (C at the center, D and E near

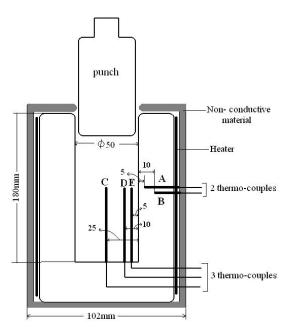


Fig. 5. Mold assembly and thermocouples position.

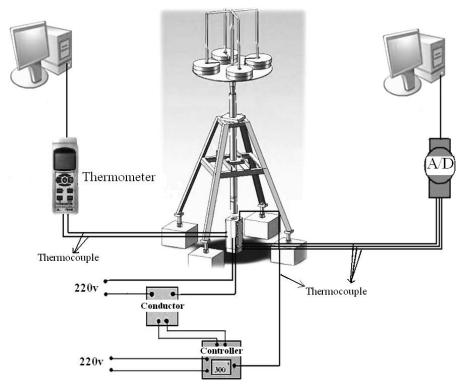


Fig. 6. Schematic representation of the experimental setup connected to the data acquisition and analysis system

the mold surface), as indicated in Figure 5.

The solution of the inverse heat conduction problem requires the use of relatively accurate experimental data. Consequently, a digital data logging system with a relatively high standard (with a PLC-32bit card, 8 channels,

Advantech corporation and SMSSmulti4018 Data logger program) of high accuracy has been supplied to record temperature data at ten reading per second (for A/D) and one reading per second (for thermometer). This data was reduced to 70 data point for each case in order to reduce the time required to run the program.

A schematic of the experimental setup for extraction of Time - Temperature curves is shown in Figure 6.

A356 al alloy was melted in an electric resistance-type furnace until the molten metal reached a predetermined temperature. Pouring temperature was approximately 730 °C (Superheat= $0.2 T_L$). The inner surface of the mold was coated with graphite at an appropriate temperature. The mold was involved in a heater and also, mold and heater were twisted in non-

conductive materials (Figure 6) and preheat temperature of the mold was held in 300 °C and became stable before pouring. It should be noted that during the melt preparation no fluxing, grain refining and degassing procedures were adopted. Loads were applied by an apparatus that was controlled by a hand crane (Figure 6) and applied 10 seconds after pouring. Maximum available load is 300 kg. During the tests all of the thermocouples were connected to data logger interfaced with computer, and temperature data were acquired automatically.

5. RESULTS AND DISCUSSION

5.1. Soundness

In the case of casting made under atmospheric pressure the shrinkage defects were confined at the top of the casting (Figure 7.a), whereas in the case of castings made under pressure, these defects were trapped within the body of the castings (Figure 7. b, c).

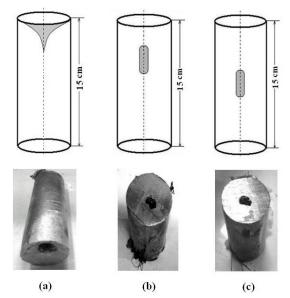


Fig. 7. Position of the shrinkages in the cast part. (a) At the top of the cast part (under atmospheric pressure); (b) Between the top and the middle of the cast part (1.14 Mpa); (c) In the middle of the cast part (1.66 Mpa).

5. 2. Time-Temperature and Heat Transfer Coefficient Evaluation

Figure 8 shows temperature curve obtained through pouring A356 Al into the mould (shown in Figure 5 without load). The thermocouples in this casting recorded oscillations in the first 5 seconds of the experiment which indicates that turbulent liquid flow in the bulk liquid alloy had occurred.

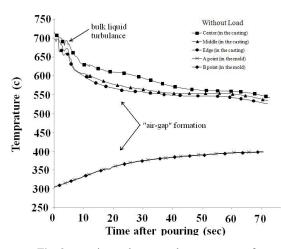


Fig. 8. experimental measured temperatures of solidification of A356 Al with time (Atmospheric).

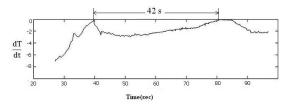


Fig.9. Derivative of the cooling curve marked as in Figure. 10 as a function of time.

The freezing time for this case (no load) was 42 seconds as shown in the derived cooling curves (Figure 9).

Using of Figure 8 and solving program flowchart Figure 3, the heat transfer coefficient for cylindrical surfaces was calculated as shown in Figure 10.

As shown in Figure 12 the empirical equations, relating interface heat transfer coefficients to the time, is:

$$h_i = 4459.t^{-0.44}$$
 (18)

The maximum heat transfer coefficients of 2885 $\left(\frac{W}{m^2k}\right)$ obtained at the cylindrical surface in no pressure application case that had good agreement with the last researches. The value of heat transfer coefficient decreases rapidly to a level of 418 in 60 seconds and then further slight decrease happens.

Figure 11 shows the temperature curves obtained through applying a load of 200kg 10 seconds after pouring.

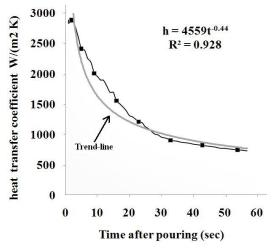


Fig. 10. The relationship between interfacial heat transfer coefficient and time (Without load).

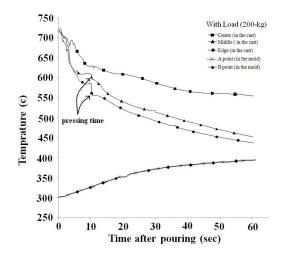


Fig. 11. Effect of pressure on the experimental measured temperatures of solidification of A356 Al with time (applied pressure =1.14Mpa).

Freezing time was 37 seconds as shown in related cooling curves (Figure 11). Compared no load case, the freezing time is very short. This means that the quantity of heat which passes through the mold casting interface becomes greater in comparison with the without load case. The sharp change in the temperature curves is attributable upon same cause.

As it was shown in Figure 11, the heat transfer coefficient for cylindrical surfaces was determined and shown in Figure 12.

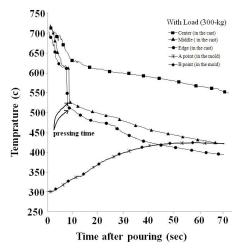


Fig. 13. Effect of pressure on the experimental measured temperatures of solidification of A356 Al with time (applied pressure =1.66Mpa).

With the application of pressure on the solidifying A356 Al metal, the heat transfer coefficient reaches maximum value of 2989 in the cylindrical surface (see Figure. 12). This value also decreases to 847.80 in 48 s.

Figure 13 shows the temperature curves obtained by applying a load of 300kg 10 seconds after pouring.

The freezing time is 34 seconds as shown in cooling curves of Figure 13.

In this case (load=300 kg), the heat transfer at

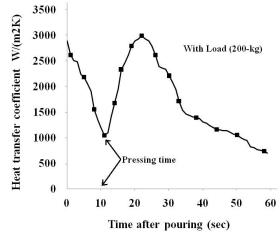


Fig. 12. Variation in interfacial heat transfer coefficient with time for A356 Al in steel mould (applied pressure =1.14Mpa).

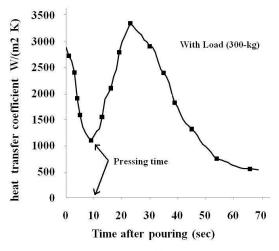


Fig. 14. Variation in interfacial heat transfer coefficient with time for A356 Al in steel mould (applied pressure =1.66Mpa).

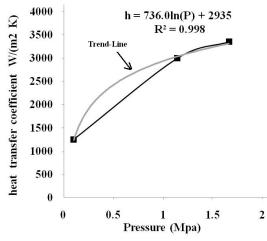


Fig. 15. Interfacial heat transfer coefficient curve versus applied pressure in 22 second.

the interface was greater than previous case (load=200 kg). By load application on the solidifying metal, the heat transfer coefficient reaches maximum value of 334 in the cylindrical surface (see Figure 14).

This value also decreases to 1000 in 48 seconds. To obtain the relationship between pressure and heat transfer coefficient in all tests, h in the 22 th second have been selected and represented by Figure 15. As shown in Figure 15 the empirical equations, relating interface heat transfer coefficients to the applied pressures, is:

6. CONCLUSIONS

Based on the results and discussion the following conclusions were drawn:

- 1. Position of the shrinkages can be changed in different pressures in the cast part. By increasing pressure, these defects shift to down and trapped within the cast part.
- 2. Heat transfer from the casting to the mold was improved considerably by applying pressure load during solidification to make good contact between mold and casting.
- 3. The transient metal/mold heat transfer coefficient (hi) have been satisfactorily determined by using the solidification temperature versus time curves obtained through varying applied pressures during

casting process.

- 4. When there is no load present on the casting, the transient metal/mold heat transfer coefficient, hi, can be expressed as a power function of time.
- 5. The empirical equations, relating interface heat transfer coefficients to the applied pressures are also derived:

7. ACKNOWLEDGEMENT

Funding for this project was provided by the Razi Metallurgical Research Center. Its support is gratefully acknowledged. The authors are grateful for the research support of the Department of materials science at Sharif University of Technology and and specially to Mr S.M.H. Mirbagheri from Department of Metallurgy, Amirkabir University of Technology.

REFERENCES

- 1. Kuo, J. H., Hsu. F. L., "Effects of mold coating and mold material on the heat transfer coefficient at the casting /mold interface for permanent mold casting of A356 aluminum alloy". AFS Transaction 2001, 01-061, 1-17.
- Ho K, Pehlke R D. "Metal–mold interfacial heat transfer". Metallurgical and Materials Transactions B,1985, 16:585–94.
- Mirbagheri, S. M. H., Shirinparvar, M., and Chirazi, A., "Modeling of metalostatic pressure on the metal mould interface thermal resistance in the casting process" Journal of Materials & Design, Volume 28, Issue 7, 2007, 2106-2112
- 4. Mirbagheri, S. M. H., "Modeling of effect of the ferrous chills and pressure on the heat transfer coefficient in metal / preheated chill interface", Material letters, Volume 62, 2008, 824–827.
- Krishnan, M., Sharma, D. G. R., "Determination of Heat Transfer Coefficient Between casting and Chill in Uni-directional Heat Flow". AFS Transaction, Vol 102 ?1994, 769.
- Santos, C. A., "Determination of transient interfacial heat transfer coefficients in chill mold castings". Journal of Alloys and Compounds 319,2001, 174–186.
- 7. Martorano, MA, Capocchi. "Heat transfer coefficient at the metal-mould interface in the

unidirectional solidification of Cu- 8%Sn alloys". Int J Heat Mass Transfer 43, 2000, 2541–2552.

- Griffiths, W. D., "A model of the interfacial heat-transfer coefficient during unidirectional solidification of an aluminum alloy". Metall Mater Trans B 31, 2000, 285–295.
- Santos, C., Quaresma, J., Garcia, A. J., "Determination of transient interfacial heat transfer coefficients in chill mold castings", Alloys Compd. 319 (2001) 174–186.
- Griffiths, W. D., "The heat transfer coefficient during the unidirectional solidification of an Al–Si alloy casting". Metall. Mater. Trans. B, vol. 30B, 1999, 473-82.
- Spinelli, J., Ferreira, I., Garcia, A., "Influence of melt convection on the columnar to equiaxed transition and microstructure of downward unsteady-state directionally solidified Sn–Pb alloys". J Alloys Compound 384, 2004, 217–226.
- Narayan, K., Ravishankar, B. N., "Effect of modification melt treatment on casting/chill interfacial heat transfer and electrical conductivity of Al-13% Si alloy", Mat. Sci. Eng.A, 360 (2003) 293–298.
- Incropera, F., Dewitt, D., "Fundamentals of Heat and Mass Transfer", 3ed. John Wiley & Sons, 1990, Singapore, 58.
- Hines, A., "Determination of Interfacial Heat-Transfer Boundary Conditions in an Aluminum Low-Pressure Permanent Mold Test Casting". Metallurgical and Materials Transactions B, Volume 35B, April 2004, 299.
- Beck, J., "Nonlinear estimation applied to nonlinear inverse heat conduction problem". Int J Heat Mass Transfer 13, 1970, 703–716.
- Loulou, T., Artyukhin, E., Bardon, J., "Estimation of thermal contact resistance during the first stages of metal solidification process: Experiment principle and modelisation". Int J Heat Mass Transfer 42, 1999, 2119–2127.
- Piwonka, T., Woodbury, K., Wiest. J., "Modeling casting dimensions: effect of wax rheology and interfacial heat transfer". Mater Des 21, 2000, 365–372.
- Nishida, Y., Matsubara. H. "Effect of Pressure on Heat Transfer at the Metal Mold-Casting

Interface". Journal of British Foundaryman, 69, 1976, 274-278.

19. Plyatskii, V., "Extrusion Casing". Primary Source, 1975, New York.